

Multi-Agent Reinforcement Learning for Network Load Balancing in Data Center

Zhiyuan Yao^{1,2*}, Zihan Ding³, Thomas Clausen¹

¹École Polytechnique

²Cisco

³Princeton University

{zhiyuan.yao, thomas.clausen}@polytechnique.edu, zhding96@gmail.com

Abstract

This paper presents the network load balancing problem, a challenging real-world task for multi-agent reinforcement learning (MARL) methods. Traditional heuristic solutions like Weighted-Cost Multi-Path (WCMP) and Local Shortest Queue (LSQ) are less flexible to the changing workload distributions and arrival rates, with a poor balance among multiple load balancers. The cooperative network load balancing task is formulated as a Dec-POMDP problem, which naturally induces the MARL methods. To bridge the reality gap for applying learning-based methods, all methods are directly trained and evaluated on an emulation system from moderate- to large-scale. Experiments on realistic testbeds show that the independent and “selfish” load balancing strategies are not necessarily the globally optimal ones, while the proposed MARL solution has a superior performance over different realistic settings. Additionally, the potential difficulties of MARL methods for network load balancing are analysed, which helps to draw the attention of the learning and network communities to such challenges.

1 Introduction

In data centers (DCs), network LBs play a significant role to distribute requests from clients across a cluster of application servers and provide scalable services [Eisenbud *et al.*, 2016a]. With the advance of virtualisation technology and elastic data centers [Dragoni *et al.*, 2017], application servers can be instantiated on heterogeneous architectures [Kumar *et al.*, 2020] and have different processing capacities. This requires network LBs to make fair workloads distribution decisions based on instant server load states to optimise resource utilisation, as shown in Figure 1, so that less application servers can be provisioned to guarantee the quality of service (QoS), with reduced operational costs. However, there are two challenges for network LBs to make fair workloads distribution decisions.

First, network LBs (LBs) have limited observations to make informed decisions. Operating at the Transport Layer, network LBs are agnostic to Application-Layer protocol and do not inspect the Application-Layer headers in network

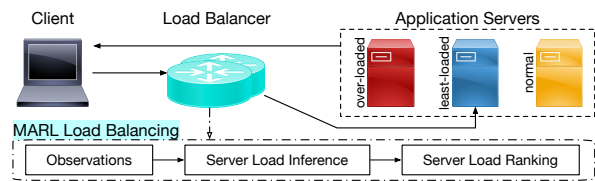


Figure 1: Network load balancing in DC networks and the scope of study of this paper.

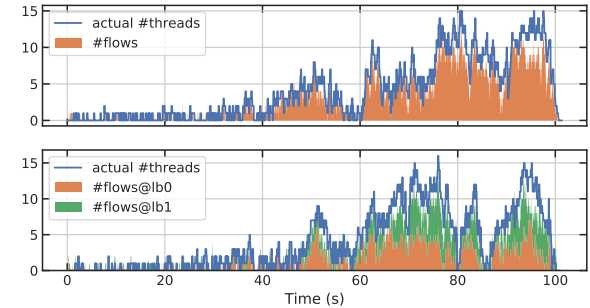


Figure 2: Comparison of the observed number of on-going flows (#flow) between single- (top) and double-load-balancer (bottom) environment.

packets, in order to generalise to all types of network applications [Eisenbud *et al.*, 2016a]. However, this makes LBs also agnostic to the information of received requests and network flows (jobs) – *e.g.*, expected job completion time (JCT) – when making load balancing decisions, which can lead to overloaded servers dealing with multiple heavy network flows [Goren *et al.*, 2020]. Besides, in modern DCs, multiple LBs are deployed to avoid single-point-of-failure and improve system reliability. Though informative features can be extracted from network packets, the presence of multiple LBs to have only partial observations on the network traffic and workloads distributed among servers. An example of partial observation of the number of on-going flows is depicted in Figure 2.

Second, network LBs deal with high flow arrival rates (higher than 500 flows/s) – load balancing decisions have to be made within sub-ms or micro-second level [Desmouzeaux *et al.*, 2018]. Reinforcement learning (RL) approaches [Chen *et al.*, 2018; Mao *et al.*, 2018; Xu *et al.*, 2019; Sivakumar *et al.*, 2019] have been proposed to address this challenge.

*Contact Author

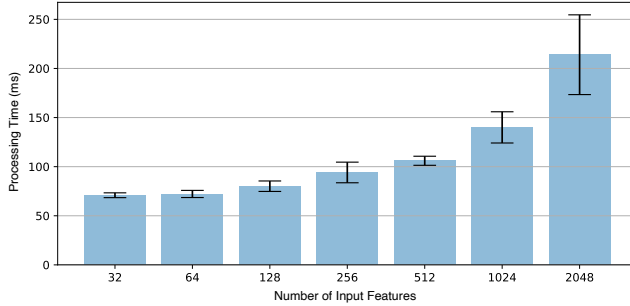


Figure 3: With a simple 3 layer fully connected neural network with 4865 parameters built with popular ML framework Keras/Tensorflow, assuming input datapoints have 32 features, it takes more than 50ms to obtain a singal output, when using single CPU core (Intel Xeon CPU E5-2690 v3 at 2.60GHz).

et al., 2019] show performance gains in various system and networking problems and help avoid error-prone manual configurations. However, Figure 3 shows that it is computationally intractable to apply RL algorithms on network load balancing problems to make more than 500 load balancing decisions per second even using a minimal size of neural network. Therefore, state-of-the-art network LBs rely on heuristics for decisions on where to place workloads [Eisenbud *et al.*, 2016b; Desmouceaux *et al.*, 2018; Aghdai *et al.*, 2018b].

This paper represents the network load balancing problem as a cooperative game to bridge the gap between the networked computing system community and MARL community. This paper proposes an asynchronous mechanism that allows to (i) take advantage of the learning and inference capacity of RL algorithms given only partial observations, and (ii) generate data-driven load balancing decisions that bring performance gains at micro-second level. Emulated environments of different scales are constructed with real-world networking traffic to evaluate and compare the proposed mechanism with state-of-the-art load balancing algorithms.

The contribution of this paper are summarised as follows: (i) This paper formally defines the network load balancing problem as a cooperative game in Dec-POMDP [Oliehoek and Amato, 2016] framework and presents an emulated environment for realistic evaluations. (ii) This paper proposes an asynchronous mechanism that allows to benefit from MARL algorithms and make sub-ms level data-driven load balancing decisions. (iii) This paper tailors a MARL algorithm QMIX [Rashid *et al.*, 2018] and a single-agent RL algorithm soft actor-critic (SAC) [Haarnoja *et al.*, 2018] as three different learning agents for solving load balancing tasks with multiple LBs, and evaluates their performance on different scenarios and compares with 5 state-of-the-art (SOTA) heuristic load balancing algorithms. (iv) By analysing the experimental results, this paper implies the possible challenges (*e.g.* scalability, synchronisation among distributed agents) for MARL to solve the network load balancing problem, and suggests future work directions.

2 Related Work

Network Load Balancing: Network LBs in modern DCs follow the distributed design as in [Eisenbud *et al.*, 2016b], where multiple LBs randomly assign servers to incoming

tasks using Equal-Cost Multi-Path (ECMP). In case where servers have different processing capacities, servers are assigned with probabilities proportional to their weights using Weighted-Cost Multi-Path (WCMP). However, as available server processing capacities change with time in DCs [Dragoni *et al.*, 2017], these statically configured weight may not correspond to the actual processing capacities of servers. As a variant of WCMP, active WCMP (AWCMP) periodically updates server weights, based on probed resource utilisation information (CPU, memory, or IO usage) [Aghdai *et al.*, 2018a; 2018b], though it requires modifications on every servers to manage communication channels and collect observations. This incurs additional control messages and management overheads, especially in large and scalable DCs. Local shortest queue (LSQ) counts the number of distributed jobs on each server [Goren *et al.*, 2020], yet it assumes that all servers share the same processing capacity. Previous work [Yao *et al.*, 2021] has explored single-agent RL for load balancing in a network systems, with a close-to heuristic performance achieved in moderate-scale simulations. For the case with multiple LBs working at the same time, this paper applies and studies MARL algorithms on the network load balancing problem in a realistic testbed to evaluate server load states based only on local observations extracted from network packets, and to dynamically adapt to time-variant environments.

MARL for Cooperative Games in Networked Computing Systems: RL has been applied on scheduling problems [Chen *et al.*, 2018; Mao *et al.*, 2018; Wu *et al.*, 2011], which is similar yet different from network load balancing problems. Agents in scheduling problems know *a priori* the information of workloads – including the expected job durations, job dependencies, etc. – to be distributed before assigning workloads to different processing queues. However, network LBs have limited observations on only the subset of network flows they distribute – only the number of flows distributed on each server and the elapsed time of on-going network flows. Comparing with the networking problems, the jobs in scheduling problems also arrive at lower rates (at second level) and have longer completion time. This paper adapts QMIX [Rashid *et al.*, 2018] in an asynchronous mechanism to make highly frequent load balancing decisions, and to learn from partial observations and solve the network load balancing problem as a cooperative game.

3 MARL Network Load Balancing

This section defines the network load balancing problem and formulates it into a cooperative game.

3.1 Multi-Agent Load Balancing Problem

Network load balancing can be defined as allocating a Poisson sequence of network flows with different workloads $w \in \mathcal{W}^1$ on a set of n servers, to achieve the maximal exploitation of the computational capacity of the servers. The workload $w^j(t)$ assigned on the j -th server at time t usually follows an exponential distribution in practical experiments [Roy *et al.*, 2015]. Multi-agent load balancing problem considers workload distribution through a number of m LBs which provide high availability and reliability in modern DCs [Eisenbud *et al.*, 2016b].

¹The unit of workload can be, *e.g.*, amount of time to process.

Deterministic Case. The load balancing method for each LB $i \in [m]$ can be a pure strategy $\pi^i \in \Pi^i: \mathcal{W} \rightarrow [n]$. Therefore, a deterministic workload assignment function is: $\mathcal{W} \times [m] \rightarrow [n]$. The ensembled policy for the whole multi-agent load balancing system is thus $\boldsymbol{\pi} = [\pi_1, \dots, \pi_m] \in \boldsymbol{\Pi} = \Pi_1 \times \dots \times \Pi_m$. The processing speed for each server is $v_j, j \in [n]$, i.e., the amount of workloads that can be processed per time time. The remaining workloads on the j -th server ($j \in [n]$) during a time interval $t \in [t_0, t_n]$ is thus defined as:

$$l_j = \frac{\sum_{i \in [m]} \sum_{t \in [t_0, t_n]} w^{i,j}(t)}{v_j}, \quad (1)$$

where $w^{i,j}(t)$ indicates the k -th workload at time t assigned to the j -th server via the i -th LB. l_j represents the expected time to finish processing all the workloads on the j -th server.

Stochastic Case. Since modern DCs have fan-out topology and $m < n$, using deterministic strategy during a time interval will flood n servers under heavy traffic rate (e.g., higher than 500 flows/s), therefore the stochastic load balancing strategies are more often used in practice [Eisenbud *et al.*, 2016b]. The stochastic workload assignment function α is defined as: $\mathcal{W} \times [m] \times [n] \rightarrow [0, 1]$, representing the probability of the event that the workload is assigned by a specific LB to a specific server. The expected time to finish of all the workloads on j -th server during the time interval $t \in [t_0, t_n]$ is, for $\forall j \in [n]$:

$$l_j = \frac{\sum_{i \in [m]} \sum_{t \in [t_0, t_n]} w^i(t) \alpha^{i,j}(t)}{v_j}, \sum_{j=1}^n \alpha^{i,j}(t) = 1 \quad (2)$$

$\alpha^{i,j}(t)$ denoting the probability that LB i choose server j for load w at time t .

Objective. The objective for the whole load balancing system can be defined as finding the optimal ensemble policy:

$$\boldsymbol{\pi}^* = \min_{\boldsymbol{\pi} \in \boldsymbol{\Pi}} c(l_1, \dots, l_n) \quad (3)$$

where c is a cost function depending on the expected task finishing time for all servers $j \in [n]$. The definition of *makespan* is $c(l_1, \dots, l_n) = \max_{j \in [n]} \{l_j\}$. However, the estimation of makespan may produce large variances when facing heavy traffic of jobs whose expected JCTs follow long-tail distribution [Roy *et al.*, 2015]. This paper thus uses a different cost function – fairness index – which is proved to be equivalent of the makespan as objective (see Appendix A).

Definition 1. (Fairness) For a vector of task completion time $\mathbf{l} = [l_1, \dots, l_n]$ on each server $j \in [n]$, the linear product-based fairness for workload distribution is defined as:

$$F(\mathbf{l}) = F([l_1, \dots, l_n]) = \prod_{j \in [n]} \frac{l_j}{\max(\mathbf{l})} \quad (4)$$

Proposition 1. Maximising the linear product-based fairness is sufficient for minimising the makespan:

$$\max F(\mathbf{l}) \Rightarrow \min \max(\mathbf{l}) \quad (5)$$

3.2 MARL Methods

The multi-agent load balancing problem defined in Eq. (3) can be viewed as a multi-agent cooperative game, where each agent needs to coordinate their behaviour to maximise the

common payoff. Specifically, each agent acts independently according to their local observations, the common payoff is improved as long as each agent improves their local policies.

Dec-POMDP. MARL for cooperative games can be formulated as decentralised partially observable Markov decision process (Dec-POMDP) [Oliehoek and Amato, 2016], which can be represented as $(\mathcal{I}, \mathcal{S}, \mathcal{A}, R, \mathcal{O}, \mathcal{T}, \gamma)$. \mathcal{I} is the agent set, \mathcal{S} is the state set and $\mathcal{A} = \times_i \mathcal{A}_i, i \in \mathcal{I}$ is the joint action set, $\mathcal{O} = \times_i \mathcal{O}_i, i \in \mathcal{I}$ is the joint observation set, and R is the global reward function $R(s, a): \mathcal{S} \times \mathcal{A} \rightarrow \mathbb{R}$ for current state $s \in \mathcal{S}$ and action $a \in \mathcal{A}$. The state-transition probability from current state and action to a next state $s' \in \mathcal{S}$ is defined by $\mathcal{T}(s'|s, a): \mathcal{S} \times \mathcal{A} \times \mathcal{S} \rightarrow [0, 1]$. $\gamma \in (0, 1)$ is a reward discount factor. The goal of the RL algorithm is optimising the joint policy $\boldsymbol{\pi} \in \boldsymbol{\Pi}$ to maximise their expected cumulative rewards: $\max_{\boldsymbol{\pi} \in \boldsymbol{\Pi}} \mathbb{E}_{\boldsymbol{\pi}} [\sum_t \gamma^t r_t]$.

QMIX. To solve the above Dec-POMDP problem, QMIX [Rashid *et al.*, 2018] algorithm is applied in the proposed method, in a centralised training but decentralised execution manner. Specifically, QMIX estimates a total Q -value function Q_{tot} as a nonlinear combination of the Q_i -value for each agent $i \in \mathcal{I}$, as long as the monotonic dependence relationship is satisfied: $\frac{\partial Q_{tot}}{\partial Q_i}, \forall i \in [\mathcal{I}]$. $Q_{tot}(\boldsymbol{\tau}, \mathbf{a}, s)$ is a function of joint action-observation history $\boldsymbol{\tau}$, joint action \mathbf{a} and the state s , while $Q_i(\tau_i, a_i)$ for each agent is a function of agent observed history τ_i and its own action a_i . The update rule of QMIX follows: $\min L = \min \sum [Q_{tot}(\boldsymbol{\tau}, \mathbf{a}, s) - (r + \gamma \max_{\mathbf{a}'} Q_{tot}(\boldsymbol{\tau}', \mathbf{a}', s'))]^2$. The agent incorporating QMIX algorithm has a stochastic policy for each LB.

SAC. For single-agent game, soft actor-critic (SAC) [Haarnoja *et al.*, 2018] follows the maximum entropy reinforcement learning framework, which optimises the objective $\mathbb{E}[\sum_t \gamma^t r_t + \alpha \mathcal{H}(\pi_\theta)]$ to encourage the exploration $\mathcal{H}(\cdot)$ of the policy π_θ during the learning process. Specifically, the critic Q network is updated using the gradients $\nabla_\phi \mathbb{E}_{s, a} [Q_\phi(s, a) - [R(s, a) + \gamma \mathbb{E}_{s'} [V_{\tilde{\phi}}(s')]]]$, where $V_{\tilde{\phi}}(s') = \mathbb{E}_{a'} [Q_{\tilde{\phi}}(s', a') - \alpha \log \pi_\theta(a'|s')]$ and $Q_{\tilde{\phi}}$ is the target Q network; the actor policy π_θ is updated using the gradients $\nabla_\theta \mathbb{E}_s [\alpha \log \pi_\theta(a|s) - Q_\phi(s, a)]$.

Independent Learning. Apart from QMIX, independent learning agents treat the objective in Eq. (3) from an independent view, where the optimal ensemble policy is factorised as the optimization over each individual policy for each LB agent:

$$\pi_i^* = \min_{\pi_i \in \Pi_i, i \in [m]} c_j(l_{i,j}), i \in [m] \quad (6)$$

where $l_{i,j} = \frac{\sum_{t \in [t_0, t_n]} w^i(t) \alpha^{i,j}(t)}{v_j}$ for the stochastic case.

The objective achieved with Eq. (6) is different from Eq. (3) unless the work loads going to each LB are exactly the same at all time, which is generally impossible in practice. SAC is used for each independent LB agent, which gives the independent-SAC (I-SAC) method.

3.3 MARL for Multi-Agent Load Balancing

The network load balancing problem is multi-commodity flow problems and is NP-hard, which makes it hard to solve with trivial algorithmic solution within micro-second level [Sen *et al.*, 2013]. In practice, limited observations on system states and changing environments require to continuously approximate server load states. This section de-

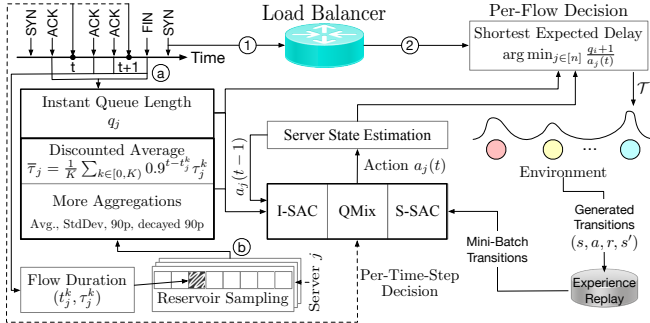


Figure 4: Overview of the proposed MARL framework for network LB. A distributed learning framework with multiple LB agents is implemented to interact with the simulated LB and allocate tasks on different servers according to a server assignment function. Each LB agent contains a replay buffer and can learn using 3 different RL algorithms – independent SAC (I-SAC), QMix, or single-agent SAC (S-SAC). The 3 RL algorithms consume the network features (on-going flows and flow duration statistics on each server) as well as the actions from last time step and generate server load state estimations as the next time-step action for making fair per-flow-level decision based on the shortest expected delay algorithm.

scribes the network load balancing problem mathematically as a cooperative Dec-POMDP under realistic constraints. The overview of the MARL framework is depicted in Figure 3.

Agent Set. There is a set of homogeneous LB agents \mathcal{I} ($|\mathcal{I}| = m$) distributing workloads among the same set of n application servers. Each agent only distributes and observes over a subset of workloads that arrive at the system.

State and Observation Set. The state set is defined as $\mathcal{S} = \mathcal{W} \times \mathcal{V}$, where $\mathcal{W} = \mathbf{w} : \mathbf{w} \in (0, \infty)^m$ is a set of incoming network traffic (workloads) to be distributed among servers, and $\mathcal{V} = \mathbf{v} : \mathbf{v} \in (0, \infty)^n$ is a set of server processing speeds. The observation set $\mathcal{O} = (\mathbf{q}, \boldsymbol{\tau}) : \mathbf{q}, \boldsymbol{\tau} \in (0, \infty)^n$, where \mathbf{q} is a vector of counting numbers, each represents the number of on-going task on each server, and $\boldsymbol{\tau}$ is a vector of statistical evaluations (mean, standard deviation, 90th-percentile, and discounted mean and 90th-percentile over time) of task elapsed time on each server.

Action Set. $\mathcal{A} = \times_i \mathcal{A}_i$ is the action set containing the individual action set \mathcal{A}_i for each agent $i \in \mathcal{I}$. In the discrete action set $\mathcal{A}_i \subset \mathbb{R}_+^n$, an action a_i is a vector representing the weights for the current workload to be allocated to n application servers by LB agent i . To make hundreds or thousands of load balancing decisions per second while incorporating RL intelligence, this paper adopts the form of the shortest expected delay (SED)² to assign server $\arg \min_{j \in [n]} \frac{q_i^j + 1}{a_i^j}$ to the

newly arrived flow, where q_i^j is the number of on-going flows on server j observed by LB i , and a_i^j is the weight assigned to server j by LB i . By tracking the number of on-going tasks on receipt of every network flow, this allows the proposed agents to make load balancing decisions at the pace of task arrival rates, which can be extremely high (\sim ms per decision) in practice. The asynchronously updated action a_i allows to approximate the changing processing speed of each server over time.

State and Observation Transition. The state transition probability function is defined as $\mathcal{T} : \mathcal{S} \times \mathcal{A} \times \mathcal{S} \rightarrow$

$[0, 1]$, following Markov decision process. More specifically, $\mathcal{T}(s_{t+1}|s_t, a_t) = \Pr(s_{t+1}|\rho(s_t, a_t))$, where $a_t \in \mathcal{A}$, $s_t, s_{t+1} \in \mathcal{S}$, $\rho(s_t, a_t) \mapsto s_{t+\delta t}$ represents the response of servers given the updated workloads distribution, and $\Pr(s_{t+1}|s_{t+\delta t})$ represents the change of incoming traffic rates and server processing speeds. The time interval between two actions, *i.e.*, a time step is denoted as $\Delta t = 250\text{ms}$ and $\delta t \ll \Delta t$.

Observation Probability Function. The observation probability function $\Omega : \mathcal{S} \times \mathcal{A} \times \mathcal{O} \rightarrow [0, 1]$ describes the measurement errors that can occur when extracting and collecting features and statistics from network packets on LB agents. The counters of on-going network flows q are subject to partial observations in presence of multiple LB agents. The flow elapsed times are collected by way of reservoir sampling (Algorithm 1 in Appendix B), which collects an exponentially-distributed number of samples over time. For a Poisson stream of events with an arrival rate λ , the expectation of the amount of samples that are preserved in buffer after T steps is $E = \lambda p \left(\frac{K-p}{K} \right)^{\lambda T}$, where p is the probability of gathering sample and K is the size of reservoir buffer. An example reservoir samples distribution over time is shown in Figure 5.

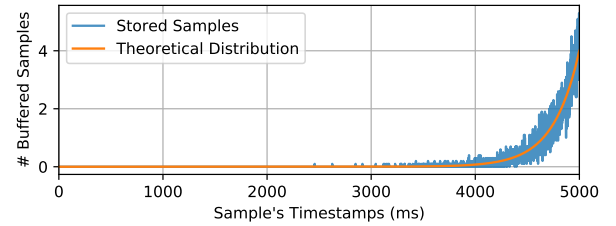


Figure 5: An example of reservoir samples' timestamp distribution with $\lambda = 80$, $p = 0.05$, $K = 10000$, $n \leq 50000$.

Reward Function. Since LB agents have limited observations over the actual server load states s , the paper uses the flow elapsed time to approximate the sum of queuing delay and task workload over the underlying processing speed of a server. To give more credits to the latest observations, given the set of samples $\{(t_j^k, \tau_j^k) | k \in [K]\}$ of server j , the discounted average of flow elapsed time (an estimation of l_j in Eq. (2)) at time t is computed as $\bar{\tau}_j(t) = \frac{1}{K} \sum_{k \in [0, K]} \gamma^{t-t_j^k} \tau_j^k$, where $\gamma = 0.9$ in this paper. Then, based on the Proposition 1, the reward function is defined as the fairness index of the exponentially weighted average of $\bar{\tau}$ for all servers:

$$r_{t+1} = \begin{cases} F(\bar{\tau}_t) & \text{if } t = 0 \\ F((1-\gamma)\bar{\tau}_t + \gamma\bar{\tau}_{t+1}) & \text{otherwise.} \end{cases} \quad (7)$$

Objective Function. The objective is to maximise their expected cumulative rewards: $\max_{\pi \in \Pi} \mathbb{E}_\pi [\sum_t \gamma^t r_t]$, through optimising over the parameterised joint policy $\pi \in \Pi$, $\pi = \times_{i \in \mathcal{I}} \pi_i$, $\pi_i : \tilde{\mathcal{O}}_i \times \mathcal{A}_i \rightarrow [0, 1]$ is the stochastic policy for agent i . $\tilde{\mathcal{O}}_i$ is a concatenation of historical observations and actions for agent i . This paper uses gated recurrent units (GRU) [Chung *et al.*, 2014] for both QMIX and SAC agents to handle the sequential history information.

²<http://www.linuxvirtualserver.org>

Table 1: Two testbed configurations.

Testbed Configuration n	Moderate Scale	Large Scale
Server Group 1	$4 \times 2\text{-CPU}$	$12 \times 4\text{-CPU}$
Server Group 2	$3 \times 4\text{-CPU}$	$12 \times 8\text{-CPU}$
LB Agents	$2 \times 8\text{-CPU}$	$6 \times 8\text{-CPU}$
Network Trace	Wikipedia Replay	Poisson Traffic
Traffic Rates	$[518.8, 796.3]$	$[391.5, 436.7]$
JCT Distribution	Real-world distribution	$\exp(200\text{ms})$

4 Experiments

To evaluate the performance of MARL LB algorithms in different realistic setups, experiments are conducted on a realistic testbed running network traces on physical servers.

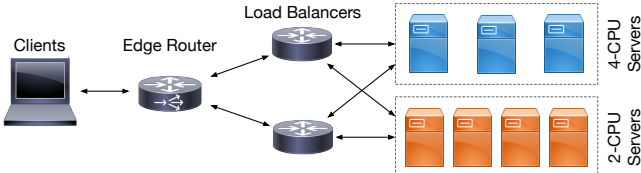


Figure 6: The moderate-scale testbed topology consisting of 1 traffic generator representing clients, an edge router, 2 LBs and 7 application servers with different processing capacities.

4.1 Experimental Settings

The experimental platform consists of VMs representing clients, an edge router, load-balancers, and Apache HTTP servers providing Web services, with the same topology as in Figure 6.

Network Settings. Two configurations are implemented to study both moderate- and large-scale DC network environments, which is noted in Table 1. In the moderate-scale testbed, network trace samples are extracted and replayed from a real-world 24-hour replay [Urdaneta *et al.*, 2009], which consists of requests for CPU-intensive Wiki pages and IO-intensive static pages. In the large-scale testbed, a synthesised Poisson traffic of CPU-intensive network flows is applied. The traffic rates of the two network traces in two different configurations are selected to consume 80% \sim 95% provisioned computational resources on average.

MARL Settings. To apply the QMIX algorithm, the action space is discretised so that the action set for each LB agent i is $\mathcal{A}_i = \{1.0, 1.2, 1.4, 1.6, 1.8, 2.0\}^n$. QMIX follows a centralised training decentralised execution manner, with each load balancer having a Q network for specifying the action choice. In order to implement the centralised training of the QMIX algorithm, TCP sockets are maintained among LB agents to create synchronised trajectories for training. The original SAC algorithm works for continuous action spaces only. Modifications are made based on [Christodoulou, 2019] to support discrete action space. The hyperparameters for

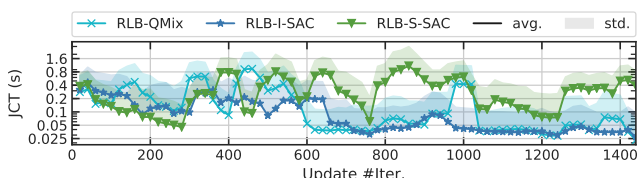


Figure 7: JCT distribution during training using 3 different RL algorithms.

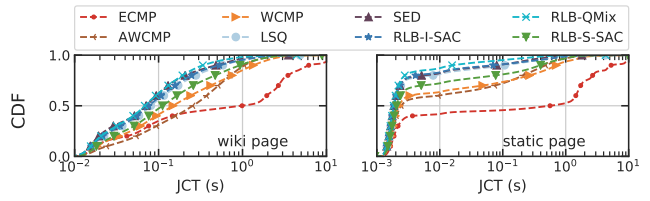


Figure 8: FCT comparison using different load balancing algorithms under different traffic rates (more than 600 queries/s, 5 runs per traffic rate).

each learning agent (QMIX, I-SAC, S-SAC) are provided in Appendix C.

Baselines. In experiments, the QMIX-based MARL (RLB-QMIX) is evaluated and compared against other methods, namely I-SAC, single-agent SAC (S-SAC), and heuristic methods including Equal-Cost Multi-Path (ECMP) [Miao *et al.*, 2017], Weighted-Cost Multi-Path (WCMP) [Eisenbud *et al.*, 2016b], active WCMP (AWCMP) [Aghdai *et al.*, 2018a], Local Shortest Queue (LSQ) [Goren *et al.*, 2020], and SED. Among these heuristics, WCMP and SED configure server weights proportional to their provisioned CPU power. For I-SAC, each load balancer has an individual SAC agent with local observations, following the independent learning manner as introduced in Section 3.2. For S-SAC, a single LB agent is deployed to process all the workloads, with a SAC algorithm for training.

4.2 Results

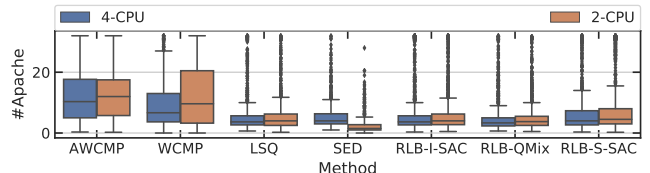


Figure 9: Comparison of number of busy Apache threads on two groups of application servers with different processing capacities.

Moderate-Scale Testbed Evaluations. As depicted in Figure 7, MARL-based LB methods show improved performance after 600 iterations of updates during training while the single agent RLB-S-SAC struggles to learn. Trained RL-based LB methods are then compared with all the heuristic LB methods on 4 unseen network traces, which covers a various range of traffic rates from 518.8 to 796.3 flows/s. As shown in Tables 2 to 5, RLB-QMIX achieves superior performance over all other methods in most scenarios, including the SOTA heuristic method (SED) and other learning agents (I-SAC and S-SAC). Only when the system is subject to the highest traffic rate (796.3 flows/s), the SED for Wiki pages and the I-SAC agents for static pages win over RLB-QMIX by a slight margin. Figure 8 depicts the overall performance comparisons by aggregating the JCTs over the 4 tested scenarios. RLB-QMIX is 1.44 \times and 5.11 \times faster than SED at 90th-percentile, which is an important QoS metric. Figure 9 shows the distribution of the number of busy Apache threads on two groups of servers. With manually configured server weights, SED assigns 2.329 \times more workloads on more powerful servers while RLB-QMIX maintains the equivalence between the two groups of servers.

Table 2: Comparison under traffic rate 518.8 flows/second.

Method	Traffic Type	
	Wiki	Static
ECMP	529.4 ± 110.5	258.6 ± 94.4
AWCMP	140.9 ± 4.1	27.6 ± 4.0
WCMP	92.6 ± 16.2	12.7 ± 8.1
LSQ	78.7 ± 29.9	8.4 ± 11.0
SED	67.2 ± 5.1	6.7 ± 3.1
RLB-I-SAC	84.3 ± 16.9	9.4 ± 7.4
RLB-QMix	63.4 ± 3.9	3.1 ± 0.1
RLB-S-SAC	84.2 ± 13.0	14.4 ± 14.4

Table 3: Comparison under traffic rate 690.9 flows/second.

Method	Traffic Type	
	Wiki	Static
ECMP	3178.9 ± 615.9	2835.3 ± 542.8
AWCMP	430.7 ± 154.5	153.3 ± 112.5
WCMP	443.6 ± 268.1	201.0 ± 188.5
LSQ	236.6 ± 164.4	69.3 ± 105.7
SED	189.3 ± 118.4	47.3 ± 48.6
RLB-I-SAC	349.6 ± 397.8	152.9 ± 260.5
RLB-QMix	166.9 ± 62.3	22.0 ± 14.1
RLB-S-SAC	397.6 ± 258.2	156.3 ± 155.9

Table 4: Comparison under traffic rate 696.5 flows/second.

Method	Traffic Type	
	Wiki	Static
ECMP	2748.5 ± 371.1	2424.6 ± 388.3
AWCMP	348.3 ± 80.3	101.3 ± 48.1
WCMP	530.7 ± 411.7	287.1 ± 355.9
LSQ	207.9 ± 67.6	40.3 ± 41.0
SED	182.6 ± 85.7	40.0 ± 35.1
RLB-I-SAC	146.4 ± 54.7	19.8 ± 16.9
RLB-QMix	88.0 ± 10.4	4.0 ± 0.7
RLB-S-SAC	169.1 ± 56.4	27.0 ± 24.1

Table 5: Comparison under traffic rate 796.3 flows/second.

Method	Traffic Type	
	Wiki	Static
ECMP	3018.5 ± 837.3	2636.8 ± 859.7
AWCMP	539.1 ± 152.4	203.6 ± 103.2
WCMP	466.8 ± 269.4	192.5 ± 181.5
LSQ	208.8 ± 117.5	50.8 ± 38.0
SED	150.9 ± 69.2	22.8 ± 18.5
RLB-I-SAC	155.0 ± 97.0	17.5 ± 21.9
RLB-QMix	188.8 ± 104.7	38.2 ± 32.1
RLB-S-SAC	398.9 ± 367.3	163.4 ± 212.3

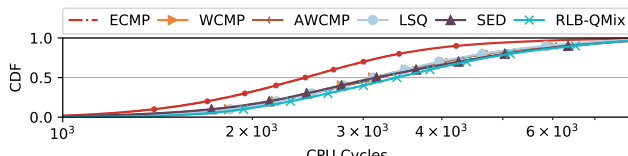


Figure 10: Load balancing decision making latency for each network flow measured under 800 flows/s traffic rate.

Large-Scale Testbed Evaluations. As shown in Table 6, although the best performances are achieved with LSQ for 398.5 flows/s traffic rate and SED for 419.3 flows/s traffic rate, MARL methods (QMIX and I-SAC) both have a very close performance to the superior method, which demonstrates a certain level of scalability for these learning-based methods to work in real-world large-scale systems.

Decision Making Latency of Asynchronous LB Framework. The decision making latency is compared among all load balancing methods on every single network flow in Figure 10. The RLB-QMIX method has 3.6% and 8.6% additional processing latency than SED and LSQ respectively. Therefore, the proposed RL framework for network load balancing problem is able to incorporate intelligence while making high-frequent decisions.

Additional experimental results including the cost of conducting centralised training in distributed systems, reasoning and analysis of baseline load balancing methods in both moderate- and large-scale experiments, can be found in the Appendix D.

Table 6: Comparison under different traffic rates (398.5, 419.3 flows/second) with synthesised CPU-intensive Poisson traffic.

Method	Traffic Rate (flows/second)	
	398.5	419.3
ECMP	5907.2 ± 550.1	7841.1 ± 484.7
AWCMP	467.7 ± 5.5	595.4 ± 6.7
WCMP	629.9 ± 25.0	1027.5 ± 65.5
LSQ	332.7 ± 1.6	420.2 ± 2.0
SED	338.6 ± 0.7	410.3 ± 2.3
RLB-I-SAC	344.8 ± 2.0	425.3 ± 1.8
RLB-QMix	340.7 ± 1.5	419.7 ± 2.8
RLB-S-SAC	353.0 ± 3.5	454.6 ± 8.4

5 Conclusions and Future Work

This paper presents a MARL framework for network load balancing problem, and evaluates different methods for the cooperative game on an emulation system. The learning-based methods including QMIX, independent-SAC and single-agent SAC are tailored for this application and compared with conventional heuristic methods. Experiments show that in moderate-scale system with different traffic rates and types, the MARL method RLB-QMIX achieve superior performance in most settings. While for large-scale system, learning agents like RLB-QMIX and I-SAC also achieve close performance to the best heuristic methods. This testify the scalability of the proposed MARL methods for real-world large-scale load balancing system. Although promising results are achieved, limitations exist in current work: (1) The QMIX algorithm makes additional structural assumption that the joint-action value is monotonic in individual agent value, which may be restrictive for the load balancing problem; (2) Reducing the communication cost among agents during training and decision making latency is important for application in real-world load balancing; (3) There are other types of scoring mechanism other than the linear-product fairness for load balancing system, like Jain's fairness etc, which is worth exploring as well. Future work includes evaluating more different types of MARL algorithms on the current system as well as a simulation system in diverse and flexible settings, to further improve the performance of MARL solutions.

References

[Aghdai *et al.*, 2018a] Ashkan Aghdai, Cing-Yu Chu, Yang Xu, David H Dai, Jun Xu, and H Jonathan Chao. Spotlight: Scalable transport layer load balancing for data center networks. *arXiv preprint arXiv:1806.08455*, 2018.

[Aghdai *et al.*, 2018b] Ashkan Aghdai, Michael I-C Wang, Yang Xu, Charles H-P Wen, and H Jonathan Chao. In-network congestion-aware load balancing at transport layer. *arXiv preprint arXiv:1811.09731*, 2018.

[Chen *et al.*, 2018] Li Chen, Justinas Lingys, Kai Chen, and Feng Liu. Auto: Scaling deep reinforcement learning for datacenter-scale automatic traffic optimization. In *Proceedings of the 2018 Conference of the ACM Special Interest Group on Data Communication*, pages 191–205. ACM, 2018.

[Christodoulou, 2019] Petros Christodoulou. Soft actor-critic for discrete action settings. *arXiv preprint arXiv:1910.07207*, 2019.

[Chung *et al.*, 2014] Junyoung Chung, Caglar Gulcehre, KyungHyun Cho, and Yoshua Bengio. Empirical evaluation of gated recurrent neural networks on sequence modeling. *arXiv preprint arXiv:1412.3555*, 2014.

[Desmouceaux *et al.*, 2018] Yoann Desmouceaux, Pierre Pfister, Jérôme Tollet, Mark Townsley, and Thomas Clausen. 6lb: Scalable and application-aware load balancing with segment routing. *IEEE/ACM Transactions on Networking*, 26(2):819–834, 2018.

[Dragoni *et al.*, 2017] Nicola Dragoni, Saverio Giallorenzo, Alberto Lluch Lafuente, Manuel Mazzara, Fabrizio Montesi, Ruslan Mustafin, and Larisa Safina. Microservices: yesterday, today, and tomorrow. In *Present and Ulterior Software Engineering*, pages 195–216. Springer, 2017.

[Eisenbud *et al.*, 2016a] Daniel E Eisenbud, Cheng Yi, Carlo Contavalli, Cody Smith, Roman Kononov, Eric Mann-Hielscher, Ardas Cilingiroglu, Bin Cheyney, Wentao Shang, and Jannah Dylan Hosein. Maglev: A fast and reliable software network load balancer. In *13th {USENIX} Symposium on Networked Systems Design and Implementation ({NSDI} 16)*, pages 523–535, 2016.

[Eisenbud *et al.*, 2016b] Daniel E Eisenbud, Cheng Yi, Carlo Contavalli, Cody Smith, Roman Kononov, Eric Mann-Hielscher, Ardas Cilingiroglu, Bin Cheyney, Wentao Shang, and Jannah Dylan Hosein. Maglev: A fast and reliable software network load balancer. In *NSDI*, pages 523–535, 2016.

[Goren *et al.*, 2020] Guy Goren, Shay Vargaftik, and Yoram Moses. Distributed dispatching in the parallel server model. *arXiv:2008.00793 [cs]*, Aug 2020. arXiv: 2008.00793.

[Haarnoja *et al.*, 2018] Tuomas Haarnoja, Aurick Zhou, Pieter Abbeel, and Sergey Levine. Soft actor-critic: Off-policy maximum entropy deep reinforcement learning with a stochastic actor. In *International conference on machine learning*, pages 1861–1870. PMLR, 2018.

[Kumar *et al.*, 2020] Adithya Kumar, Iyswary Narayanan, Timothy Zhu, and Anand Sivasubramaniam. The fast and the frugal: Tail latency aware provisioning for coping with load variations. In *Proceedings of The Web Conference 2020*, pages 314–326, 2020.

[Mao *et al.*, 2018] Hongzi Mao, Malte Schwarzkopf, Shaileshh Bojja Venkatakrishnan, Zili Meng, and Mohammad Alizadeh. Learning scheduling algorithms for data processing clusters. *arXiv preprint arXiv:1810.01963*, 2018.

[Miao *et al.*, 2017] Rui Miao, Hongyi Zeng, Changhoon Kim, Jeongkeun Lee, and Minlan Yu. Silkroad: Making stateful layer-4 load balancing fast and cheap using switching asics. In *Proceedings of the Conference of the ACM Special Interest Group on Data Communication, SIGCOMM ’17*, page 15–28. ACM, 2017. event-place: Los Angeles, CA, USA.

[Oliehoek and Amato, 2016] Frans A Oliehoek and Christopher Amato. *A concise introduction to decentralized POMDPs*. Springer, 2016.

[Rashid *et al.*, 2018] Tabish Rashid, Mikayel Samvelyan, Christian Schroeder, Gregory Farquhar, Jakob Foerster, and Shimon Whiteson. Qmix: Monotonic value function factorisation for deep multi-agent reinforcement learning. In *International Conference on Machine Learning*, pages 4295–4304. PMLR, 2018.

[Roy *et al.*, 2015] Arjun Roy, Hongyi Zeng, Jasmeet Bagga, George Porter, and Alex C. Snoeren. Inside the social network’s (datacenter) network. In *Proceedings of the 2015 ACM Conference on Special Interest Group on Data Communication, SIGCOMM ’15*, page 123–137. ACM, 2015. event-place: London, United Kingdom.

[Sen *et al.*, 2013] Siddhartha Sen, David Shue, Sunghwan Ihm, and Michael J Freedman. Scalable, optimal flow routing in datacenters via local link balancing. In *Proceedings of the ninth ACM conference on Emerging networking experiments and technologies*, pages 151–162, 2013.

[Sivakumar *et al.*, 2019] Viswanath Sivakumar, Tim Rocktäschel, Alexander H Miller, Heinrich Küttler, Nantas Nardelli, Mike Rabbat, Joelle Pineau, and Sebastian Riedel. Mvfst-rl: An asynchronous rl framework for congestion control with delayed actions. *arXiv preprint arXiv:1910.04054*, 2019.

[Urdaneta *et al.*, 2009] Guido Urdaneta, Guillaume Pierre, and Maarten van Steen. Wikipedia workload analysis for decentralized hosting. *Elsevier Computer Networks*, 53(11):1830–1845, July 2009.

[Wu *et al.*, 2011] Jun Wu, Xin Xu, Pengcheng Zhang, and Chunming Liu. A novel multi-agent reinforcement learning approach for job scheduling in grid computing. *Future Generation Computer Systems*, 27(5):430–439, 2011.

[Xu *et al.*, 2019] Yue Xu, Wenjun Xu, Zhi Wang, Jiaru Lin, and Shuguang Cui. Load balancing for ultra-dense networks: A deep reinforcement learning based approach. *IEEE Internet of Things Journal*, 6(6):9399–9412, Dec 2019. arXiv: 1906.00767.

[Yao *et al.*, 2021] Zhiyuan Yao, Zihan Ding, and Thomas Heide Clausen. Reinforced workload distribution fairness. *arXiv preprint arXiv:2111.00008*, 2021.

A Proof of Proposition 1

For a vector of task completion time $\mathbf{l} = [l_1, \dots, l_n]$ on each server $j \in [n]$, by the definition of fairness,

$$\max F(\mathbf{l}) = \max \frac{\prod_{j \in [n]} l_j}{\max_{k \in [n]} l_k} \quad (8)$$

WLOG, let $l_k = \max_{k \in [n]} l_k$, then,

$$\max F(\mathbf{l}) = \max \prod_{j \in [n], j \neq k} l_j \quad (9)$$

By means inequality,

$$\left(\prod_{j \in [n], j \neq k} l_j \right)^{\frac{1}{n-1}} \leq \frac{\sum_{j \in [n], j \neq k} l_j}{n-1} = \frac{C - l_k}{n-1}, C = \sum_{j \in [n]} l_j. \quad (10)$$

with the equivalence achieved when $l_i = l_j, \forall i, j \neq k, i, j \in [n]$ holds. Therefore,

$$\max F(\mathbf{l}) \Rightarrow \max \frac{C - l_k}{n-1} \quad (11)$$

$$\Leftrightarrow \min l_k \quad (12)$$

$$\Leftrightarrow \min \max_{j \in [n]} l_j \quad (13)$$

The inverse may not hold since $\max \frac{C - l_k}{n-1}$ does not indicates $\max F(\mathbf{l})$, so maximising the linear product-based fairness is sufficient but not necessary for minimising the makespan. This finishes the proof.

B Reservoir Sampling Algorithm

The reservoir sampling algorithm is presented

Algorithm 1 Reservoir sampling

```

1:  $K \leftarrow$  reservoir buffer size
2:  $p \leftarrow$  probability of gathering samples
3:  $buf \leftarrow [(0, 0), \dots, (0, 0)]$   $\triangleright$  Size of  $K$ 
4:  $M \leftarrow \frac{1}{p}$ 
5: for each observed sample  $v$  arriving at  $t$  do
6:    $randomId \leftarrow rand()$ 
7:   if  $randomId \% M == 0$  then
8:      $idx \leftarrow randomId \% N$   $\triangleright$  randomly select one index
9:      $buf[idx] \leftarrow (t, v)$   $\triangleright$  register sample in buffer

```

C Hyperparameters and Training Details

RL-based load balancing methods are trained in both moderate- and large-scale testbed setups for 72 episodes. At the end of each episode, the RL models are trained and updated for 25 iterations. Given the total provisioned computational resource, the traffic rates of network traces for training are carefully selected so that the RL models can learn from sensitive cases where workloads should be carefully placed to avoid overloaded less powerful servers. The traffic rates for large-scale setup is lower than the one for moderate-scale setup (see Table 1), because the synthesised Poisson traffic has heavier per-job workloads than the real-world Wikipedia Web trace.

Table 7: Hyperparameters in MARL-based LB.

	Hyperparameter	Values
Moderate-Scale	Learning rate	1×10^{-3}
	Batch size	12
	Replay Buffer Size	3000
	Episodes	72
	Episode Length	60s
	Step Interval	0.25s
	Update Iterations	0.25s
Large-Scale	Target Entropy (SAC)	$- \mathcal{A} $
	Learning rate	3×10^{-4}
	Batch size	12
	Replay Buffer Size	3000
	Episodes	72
	Episode Length	30s
	Step Interval	0.25s
	Target Entropy (SAC)	$- \mathcal{A} $

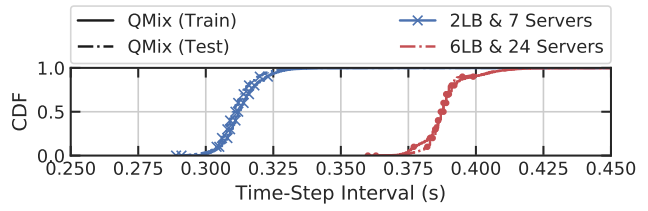


Figure 11: Time-step interval is incremented when using QMIX because of the synchronisation process.

D Additional Experimental Results

Centralised Training and Communication Overhead. QMIX adopts the centralised training scheme, which is challenging to implement in an emulated distributed system. This paper synchronises all the LB agents by way of TCP connections among all agents. Only one agent takes the responsibility of orchestrating the actions of the other agents so that the interactions between agents and the environments are synchronised and the gathered trajectories follows the Dec-POMDP specification. This implementation shows good performance in this paper, especially in the moderate-scale setup. However, in the large-scale setup, RLB-QMIX is outperformed by SED and LSQ with a small margin. One of the reasons is that the increased communication overhead (latency) and delayed actions at the presence of more LB agents. As depicted in Figure 11, in the large-scale setup, the time interval between two consecutive controls (actions) is 1.24× larger than in the moderate-scale setup. Future studies need to be conducted to alleviate this issue.

More Analysis for Baseline LB Methods. Among all the heuristic LB methods, SED has the best performance since it takes both the queue occupation and server processing capacity information into account. However, when there are multiple LB agents, SED will be mis-guided because of the partially observed numbers of on-going flows. In the large-scale setup, as depicted in Figure 12, SED assigns 2.67× and 2.25× more workloads to more powerful servers under 398.5 and 419.3 flows/s traffic rates, while the capacity ratio between the two groups of servers is 2. This behavior will lead to overloaded powerful servers, which is the reason why LSQ performs better than SED with low traffic rates. Future stud-

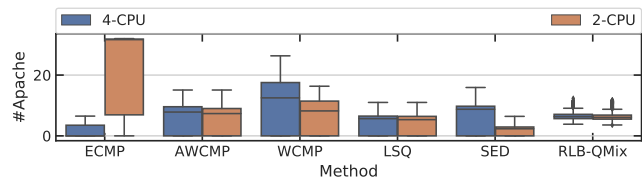


Figure 12: Comparison of the distribution of busy Apache threads on two groups of servers with different processing speeds in the large-scale scenario.

ies need to be conducted to learn and adapt to use different strategies under different scenarios.